JOURNAL OF MATERIALS SCIENCE **34** (1999) 215–227

Creep of CaO/SiO_2-containing MgO refractories*

A. A. WERESZCZAK, T. P. KIRKLAND
High Temperature Materials Laboratory, Oak Ridge National Laboratory, Oak Ridge, TN 37831-6069

W. F. CURTIS
Glass Technology Center, PPG Industries, Inc., Pittsburgh, PA 15238-0472

Compressive creep of five commercially-available brands of CaO/SiO_2-containing MgO refractories was measured over a temperature range of 1400–1550 °C and compressive stresses of 0.10–0.30 MPa. All brands had a MgO content greater than 96 wt %, a CaO/SiO_2 wt % ratio equal to or greater than 1.9, and a firing temperature greater than 1535 °C. The more creep resistant brands were observed to have a combination of: (1) a larger average grain size and wider grain size distribution, (2) a low iron content, and (3) an absence of CaO-MgO-SiO_2 compounds. Creep-stress exponents for three of the five brands indicated their creep was rate-controlled by diffusion, and their activation energy values indicated that creep was accommodated by grain boundary sliding through viscous flow of the calcium silicate grain-boundary phase. Two brands exhibited dramatic time-hardening behavior which resulted in their creep not being well-represented by the power-law creep formulation. The observed attributes among the brands were combined and a hypothetical CaO/SiO_2-containing MgO refractory is proposed.

1. Introduction

Calcia-silicate (CaO/SiO_2)-containing magnesium oxide (MgO) refractories are widely used in soda-lime glass furnace regenerators because of their good corrosion resistance to the alkaline environment. High-fired, high-purity MgO offers improved creep resistance over their lower-purity MgO counterparts. A better creep resistance is advantageous because thicker insulation (in the case of the use of MgO use in a furnace crown) can be used while maintaining structural integrity which consequentially results in greater energy savings [1]. However, regenerator checker settings (see Fig. 1) and crown applications are susceptible to creep deformation during service because they are subjected to compressive stresses at high temperatures. The compressive loading in crowns results from their arch-shaped construction, while that in the regenerator settings results from the vertical stacking. Consequently, the use of a creep-resistant refractory material is a requirement for optimum service life and performance in these applications.

A great deal of understanding has resulted from the high temperature mechanical characterization of "high-purity" magnesium oxide refractories sintered with calcium silicates over the last twenty years. Snowden and Pask [2] tested a $CaO/MgO/SiO_2$ refractory and observed a change in creep mechanism from dislocation motion at 1200 °C to viscous deformation at 1450 °C. Dixon-Stubbs and Wilshire [3, 4] performed several systematic compressive creep studies on various single and polycrystalline MgO materials in the early 1980s. They investigated a high purity (99.85%) polycrystalline MgO material at temperatures up to 1323 °C (2413 °F) at relatively high compressive stresses (68 MPa or ≈10 ksi). The determined activation energy value ($Q \approx 460$ kJ/mol ≈ 110 kcal/mol) and a stress exponent value ($n \approx 3$) were indicative of creep deformation which was rate limited by diffusion-controlled generation of dislocations [3]. Dixon-Stubbs and Wilshire [4] also examined a commercial MgO refractory (>95% MgO, a CaO/SiO_2 wt % ratio of 2.75) between 1247 °C (2275 °F) and 1337 °C (2440 °F) at relatively low stresses (≈1 to 4.3 MPa or ≈350 to 630 psi). An activation energy of 350 kJ/mol (≈83 kcal/mol) and a stress exponent approximately equal to unity indicated that the rate limiting mechanism of creep at those test conditions was stress-directed vacancy diffusion along grain boundaries (i.e., Coble creep). Ghose and White [5] examined the high temperature strength of a MgO refractory and determined that the high temperature modulus of rupture was maximized if the CaO/SiO_2 wt % ratio was approximately equal to two. Evans *et al*. [6] compressively-crept a high purity MgO refractory (99.85%) up to 1500 °C (2730 °F) and 4.3 MPa (≈630 psi) to examine the grain size distribution and impurity effects. No

* Research sponsored by the U.S. Department of Energy, Assistant Secretary for Energy Efficiency and Renewable Energy, Office of Transportation Technologies, as part of the High Temperature Materials Laboratory User Program under Contract DE-AC05-96OR22464, managed by Lockheed Martin Energy Research Corporation.

‡ Member, American Ceramic Society.

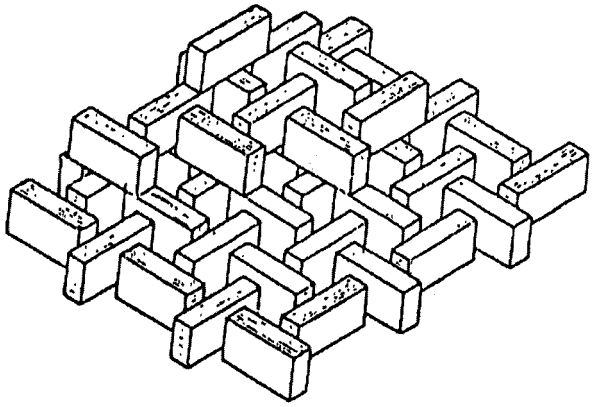

Open Basket Weave Construction

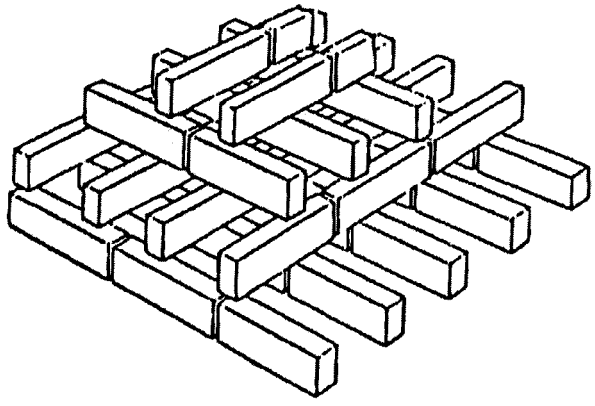

Straight Pigeon Hole Packing

Figure 1 An example of regenerator checker settings used in glass furnace regenerators.

dependence of the grain size distribution on the creep response was observed, while the reduction of impurity levels, particularly Fe_2O_3, was found to significantly improve creep resistance. Vasilos *et al*. [7] performed flexure creep testing on a fine-grained, high purity MgO between 1180 and 1260 °C (2155 and 2300 °F) and determined an activation energy of ≈310 kJ/mol (≈74 kcal/mol).

Reasons why the data and information reported in these above articles are not readily amenable for use in the design of regenerator structures are because (1) MgO refractory creep data are lacking over the temperature and (2) stress ranges typical of regenerator service conditions in glass manufacturing furnaces. Further motivation for the present study is the fact that it is difficult for the end user to make equitable and confident comparisons of the high temperature deformation behavior among the various brands of high MgO refractories. The difficulties to make comparisons arise because different test methods are used by the refractory suppliers which are not truly correlatable. For example, some suppliers may use a somewhat common refractory deformation test method which involves loading a specimen at a predefined compressive stress for 50 hours [8], whereas other suppliers conduct compressive creep tests with a continuous measurement of specimen contraction.

For the present study, five commercially available candidate CaO/SiO_2-containing MgO refractory brands for regenerator applications were compressive creep tested at representative service temperatures and stresses. An identical testing protocol in which compressive creep strain was continuously monitored as a function of time was employed for all brands. The creep rate for each brand was determined and explored as a function of stress and temperature. Explanations of different creep rate differences were sought as a function of their respectively different MgO contents, CaO/SiO_2 ratios, grain size distributions, secondary phases, and porosity. The physical and chemical character of a hypothetical CaO/SiO_2-containing MgO refractory is then proposed based on the findings in the present study.

2. Experimental

2.1. Characterization of materials

Five commercially-available brands of CaO/SiO_2-containing MgO refractories produced by five different vendors were examined. The five brands were designated in the present study as materials 'A', 'B', 'C', 'D', and 'E', due to a desire to maintain their anonymity. All contained a calcium silicate as the secondary phase. All brands were fired at tempertures in excess of 1535 °C (2800 °F) according to the vendors' technical literature. Average density, porosity, and specific gravity were measured from three core specimens from each brand using a boiling water method according to ASTM C20 [9].

Grain size distributions were measured in the five as-received MgO refractories. Sectioned and metallographically polished specimens were prepared and used to measure grain size. The sizes of a minimum of 100 grains in each brand were used to calculate a mean, standard deviation, and a median. An example of the grain structure is shown in Fig. 2a. The larger MgO grains (see Fig. 2b) were comprised by smaller crystals. Although the MgO crystal sizes were not quantitatively measured, these crystals within the grains ranged in size between 20 and 100 μm for all five brands. Optical microscopy was used for the grain size measurements, and was able to resolve grain sizes larger than approximately 0.12 mm (0.005 in.).

Phase analysis was performed on each of the five brands using X-ray diffraction (XRD). An as-received specimen from each of the five brands was examined. The metallographically prepared specimens used for the agglomerate size measurements were used for the XRD analysis. The samples were scanned at a rate of 1°/min with CuK_α radiation ($\lambda = 1.54059$ Å), and a step size of 0.02° over a scan range of 10 to 120° two-theta.

Lastly, energy dispersive spectroscopy (EDS) in a field-emission scanning electron microscope (SEM) (FE-SEM S-4100, Hitachi, Tokyo, Japan) was used to qualitatively determine the chemistry in the agglomerate boundaries in the five as-received brands. The EDS system was able to identify elements whose atomic concentration was greater than approximately 100 ppm (0.01%).

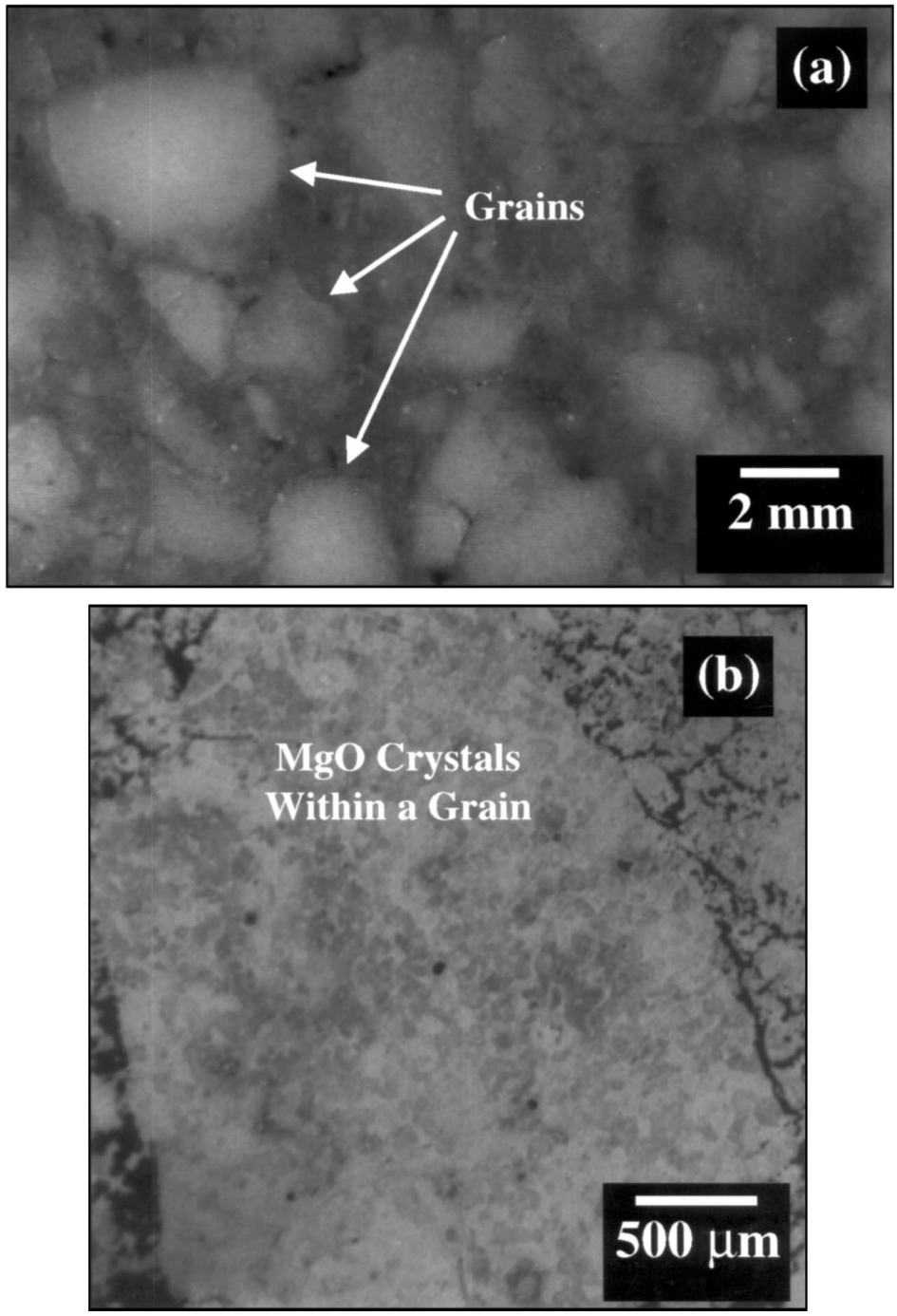

Figure 2 A representative example of the (a) grain structure in the MgO refractories and (b) crystal structure within the grains. Material A polished surfaces shown.

2.2. Creep testing

Cylindrical test specimens (nominal dimensions: 38 mm diameter $\times$ 76 mm length) were core drilled from as-received bricks. The primary axis of the machined cylinder-shaped specimens was oriented parallel to the pressing direction. Although not verified in the present study, the measured creep deformation was assumed to be isotropic because creep deformation in other MgO refractories has been shown to be largely independent of direction within a pressed brick [4]. After core drilling, the specimen ends were ground parallel to within 0.013 mm. Three specimens of each brand were prepared. A specimen aspect ratio of 2.6 or greater is recommended for *compressive strength tests* so that the friction effects between the specimen ends and loading ram are small compared to the axially applied compressive stresses [10]. However, in the present study (aspect ratio = 2.0), the applied axial compressive stresses during creep testing were already low (i.e., much less than the refractories' compressive strengths). Consequently, the stresses and strains due to such friction were likely negligible, so adherence to the height/diameter ratio of 2.6 or greater was deemed unnecessary.

Creep tests were performed in ambient air using an electromechanical test machine (Model 6027, Instron Inc., Canton, MA) in load control. The load train consisted of concentrically aligned sintered α-SiC (Hexaloy SA^{TM}, Carborundum Co., Niagara Falls, NY)

TABLE I Test matrix for the compressive creep tests

MgO refractory ID	Stresses (MPa)		
	1400 °C or 2550 °F	1475 °C or 2685 °F	1550 °C or 2820 °F
A	0.1, 0.2, and 0.3	0.1, 0.2, and 0.3	0.03, 0.1, 0.2, and 0.3
B	0.1, 0.2, and 0.3	0.1, 0.2, and 0.3	0.03, 0.1, 0.2, and 0.3
C	0.1, 0.2, and 0.3	0.03, 0.1, 0.2, and 0.3	0.03, 0.1, 0.2, and 0.3
D	0.1, 0.2, and 0.3	0.03, 0.1, 0.2, and 0.3	0.03, 0.1, 0.2, and 0.3
E	0.1, 0.2, and 0.3	0.03, 0.1, 0.2, and 0.3	0.03, 0.1, 0.2, and 0.3

Note 1: The amount of sintering-induced-contraction was only measured with the 0.03 MPa stress. A creep rate for this stress was not determined.
Note 2: Stress conversions: 0.03 MPa = 4 psi; 0.1 MPa = 14.5 psi; 0.2 MPa = 29.0 psi; and 0.3 MPa = 43.5 psi.

push rods which were surrounded by a resistance-heated clamshell furnace (Model 3320, Applied Test Systems, Inc., Butler, PA) High purity (99.5%) alumina disks (≈3 mm thick) were inserted between the specimen ends and the push rods to prevent reaction between them. A high-temperature contacting extensometer was used to continuously measure specimen contraction due to the compressive load. The extensometer's contacting rods were made of sapphire (Saphikon Inc., Milford, NH), and did not react or fuse to the MgO specimens during any of the creep tests. The extensometer had a gauge length of 40.00 mm (1.575 in.) and its resolution was approximately 1 μm (0.00004 in.) at temperature. All specimens were preloaded to approximately 0.03 MPa (≈4 psi) during furnace heatup to keep all the load train components and specimen in continuous contact. Each of the specimens were soaked at temperature for approximately 15–20 hours prior to the application of the first stress.

A total of 15 specimens were tested and the test matrix is shown in Table I. One specimen from each brand was tested at 1400 °C (2550 °F), 1475 °C (2685 °F), and 1550 °C (2820 °F). Within ASTM guidelines [11], temperature fluctuations were approximately ±2 °C and load fluctuations were less than 1% of test load. All specimens were loaded sequentially at three stresses: 0.1, 0.2, and 0.3 MPa (14.5, 29.0, and 43.5 psi) for approximately 75 hours at each stress. The repeatability in the creep performances of like-brand-specimens is unknown because only one specimen per condition was examined. Part way through the completion of the test matrix, it was observed that many of the specimens exhibited significant contraction *during the heatup and soak steps.* For the remainder of the test matrix, this specimen contraction (an apparent compressive strain) was measured continuously.

2.3. Analysis of creep data

The steady-state or minimum compressive creep rate ($d\varepsilon/dt_{min}$) was related to the applied compressive stress and temperature using an Arrhenius power law or the familiar Norton-Bailey creep equation [12]:

$$d\varepsilon/dt_{min} = A\sigma^n \exp(-Q/RT), \quad (1)$$

where A is a constant, σ is the stress, n is the applied stress exponent, Q is the activation energy, R is the gas constant, and T is the absolute temperature. Multilinear regression was performed to determine the constants A, n, and Q for each brand of MgO refractory. By performing the analysis in this manner, it is implied the same dominant (or rate-controlling) creep mechanism is active at all temperatures and stresses. The validity of this assumption is assessed by the goodness-of-fit of this equation to the experimental data and the reasonableness of the obtained values for n and Q.

3. Results and discussion

3.1. Character of as-received materials

MgO content, wt % CaO/SiO_2, density, and porosity data for each of the five brands are shown in Table II. All five refractories contained greater than 96 wt % MgO and had CaO/SiO_2 wt % ratios equal to or greater than 1.9. The MgO-SiO_2-CaO ternary [13] and SiO_2-CaO binary [14] phase diagrams are shown in Fig. 3a and b, respectively, as reference. The vendors use a CaO/SiO_2 wt % ratio in excess of 1.86 to promote the formation of the dicalcium and tricalcium silicate phases (and their relatively high eutectic temperature of 2050 °C). Note that a CaO/SiO_2 wt % ratio less than 1.86 results in a dramatic decrease in the liquid-phase-formation temperature (1464 °C

TABLE II Property comparison of MgO refractories

Property	Material				
	A	B	C	D	E
MgO (wt %)[a]	98.5	96.1	96	97.5	96.1
CaO/SiO_2 (wt %/wt %)[a]	2.7	1.9	2.0	2.3	1.9
Measured density [9]	2.93 g/cc 183 pcf	2.96 g/cc 185 pcf	2.98 g/cc 186 pcf	2.96 g/cc 185 pcf	3.00 g/cc 187 pcf
Measured porosity (%) [9]	16.1	16.1	15.5	16.2	14.9
Measured apparent specific gravity [9]	3.50	3.54	3.52	3.54	3.52

[a]Manufacturer's reported data.

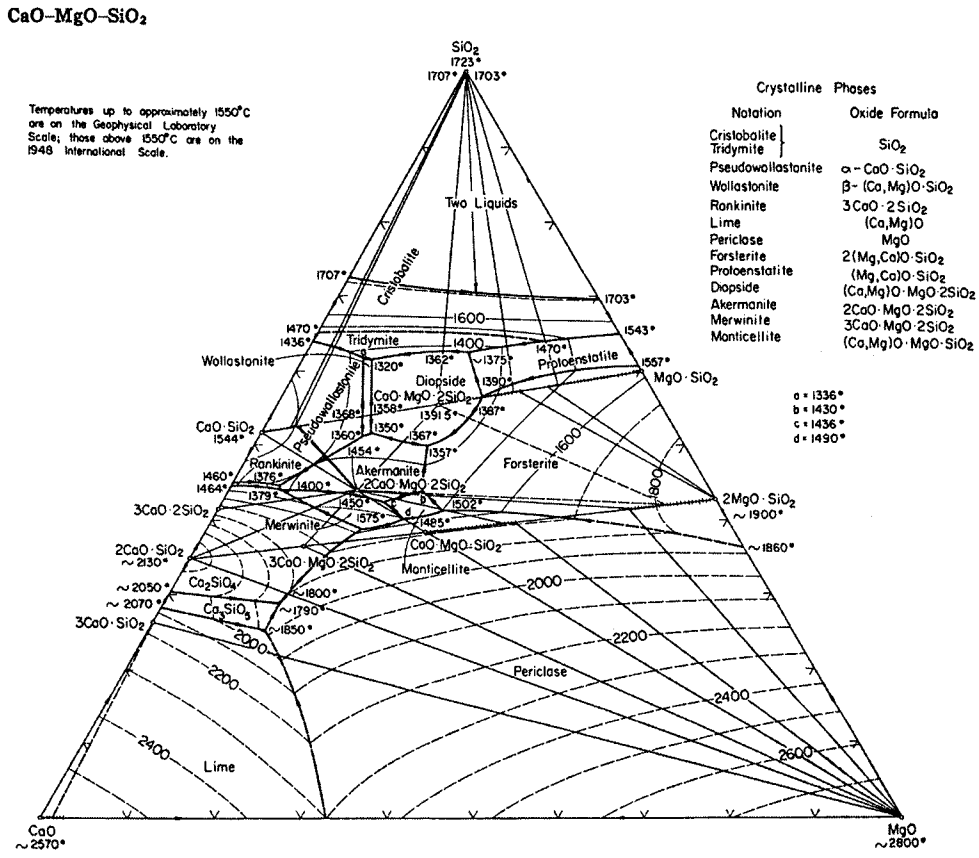

(a)

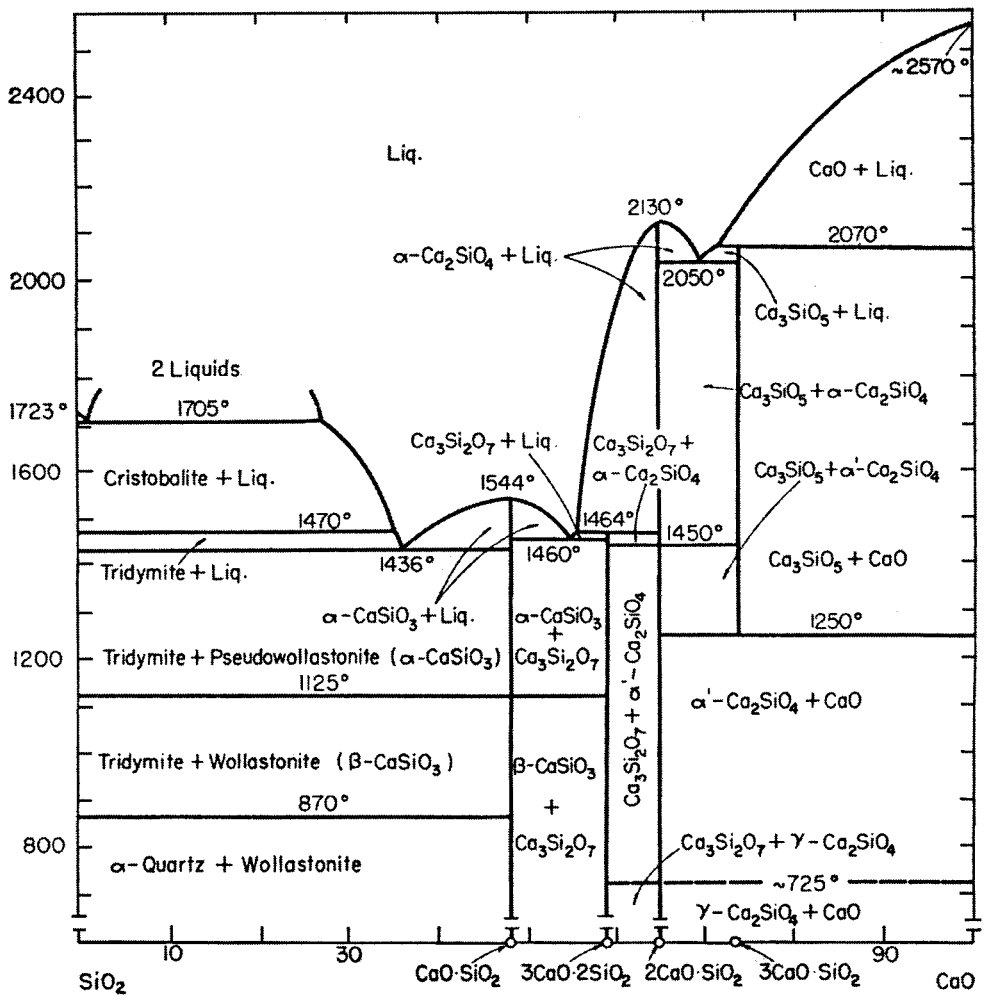

(b)

Figure 3 Phase diagrams of (a) the MgO-SiO_2-CaO ternary system [13], and (b) the SiO_2-CaO binary system [14].

peritectic). Additionally, these higher-valued ratios of CaO/SiO_2 phases also show less tendency to wet the MgO crystals than the lower CaO/SiO_2 ratio phases. Consequently, silicate phase migrates to pockets between crystals during processing resulting in a relatively high degree of solid-solid bonding between adjacent MgO crystals (see Fig. 2b). The measured density and determined porosity for each of the five brands were equivalent.

The determined grain size distributions for the five brands are shown in Table III. The average grain sizes for materials A and E were significantly larger than those for the other three brands. Many of the grains in materials A and E were non-equiaxed or acicular in shape, whereas the grains in materials B, C, and D were more equiaxed in shape. Lastly, the grain size distribution was significantly wider for material E than the other four brands.

TABLE III Grain size distributions of the as-received MgO refractories. Only grains larger than 0.012 mm were measured

MgO refractory ID	Average size (mm)	Standard deviation (mm)	Median (mm)	Maximum size (mm)
A	1.66	0.86	1.40	4.45
B	1.02	0.65	0.91	3.56
C	1.25	0.90	0.89	3.94
D	1.00	0.59	0.90	3.81
E	1.54	1.29	1.27	8.51

The XRD results generated from the as-received materials showed differences in phase content among them, and they are tabulated in Table IV. All five brands showed the presence of Periclase (MgO), magnesium silicate ($MgO{\cdot}SiO_2$), dicalcium silicate ($2CaO{\cdot}SiO_2$), and tricalcium silicate ($3CaO{\cdot}SiO_2$). The presence of the di- and tricalcium silicates supports the vendors' supplied data with respect to the CaO/SiO_2 wt % >1.86 and its subsequent propensity to form these phases (see Fig. 3b). Materials B, C, and D also contained Merwinite ($3CaO{\cdot}MgO{\cdot}2SiO_2$) or Monticellite ($CaO{\cdot}MgO{\cdot}SiO_2$). The peaks for these two phases are similar and were indistinguishable due to their low measured intensities and diffuse bandwidths. Lastly, material D contained forsterite ($2MgO{\cdot}SiO_2$) and an undetermined phase (peak at $2\theta = 27.36^\circ$). None of the five brands contained lime (CaO), Wollastonite ($CaO{\cdot}SiO_2$), Rankinite ($3CaO{\cdot}2SiO_2$), Akermanite ($2CaO{\cdot}MgO{\cdot}2SiO_2$), Bredigite ($14CaO{\cdot}MgO{\cdot}8SiO_2$), or Brucite ($Mg(OH)_2$).

Energy dispersive spectroscopy results shown in Table V did not reveal significant differences among the five brands with the exception of material D. The presence of iron (greater than 100 ppm or 0.01%) was

TABLE IV Phase analysis of as-received MgO refractories

	Material				
Phase[a]	A	B	C	D	E
Periclase MgO PDF#45-0946	×	×	×	×	×
Magnesium silicate $MgO{\cdot}SiO_2$ PDF#34-1216	×	×	×	×	×
Forsterite $2MgO{\cdot}SiO_2$ PDF#35-0590				× (weak)	
Dicalcium silicate $2CaO{\cdot}SiO_2$ PDF#31-0297	× (weak & diffuse)	× (weak & diffuse)	× (weak & diffuse)	× (weak & diffuse)	× (weak & diffuse)
Tricalcium silicate $3CaO{\cdot}SiO_2$ PDF#31-0301	× (strong)	× (weak)	× (strong)	× (strong)	× (weak)
Rankinite $3CaO{\cdot}2SiO_2$ PDF#22-0539					
Monticellite $CaO{\cdot}MgO{\cdot}SiO_2$ PDF#35-0590 or Merwinite $3CaO{\cdot}MgO{\cdot}2SiO_2$ PDF#35-0591[b]		× (weak & diffuse)	× (weak & diffuse)	× (weak & diffuse)	
Undetermined peak at $2\theta = 27.36^\circ$				× (weak)	
Undetermined peak at $2\theta = 34.20^\circ$					

[a]These phases were also sought but were not found: Lime (CaO – PDF#37-1497); Wollastonite ($CaO{\cdot}SiO_2$ – PDF#43-1460); Akermanite ($2CaO{\cdot}MgO{\cdot}2SiO_2$ – PDF#35-0592); Bredigite ($14CaO{\cdot}MgO{\cdot}8SiO_2$ – PDF#36-0399); and Brucite ($Mg(OH)_2$ – PDF#07-0239).
[b]The primary peaks for these two phases are similar and were indistinguishable because their intensities were low-valued and diffuse.

TABLE V EDS qualitative analysis of grain boundary phase. A checkmark indicates that a concentration in excess of 100 ppm (0.01%) was detected

Element	Material				
	A	B	C	D	E
O(Kα)	×	×	×	×	×
Fe (Lα1)				×	
Na (Kα)	×	×	×	×	×
Mg (Kα)	×	×	×	×	×
Al (Kα)	×	×	×	×	×
Si (Kα)	×	×	×	×	×
Ca (Lα1)	×	×	×	×	×

uniquely detected in material D. Once this was observed, the undetermined XRD $2\theta = 27.36^\circ$ peak for material D was reexamined; however, oxides of iron in combination with the other elements shown in Table V did not reveal any peaks coincident with this 2θ value, so this peak remained unidentified. All five brands contained sodium and aluminum. The quantitative amounts of sodium and aluminum were not determined, but their presence in glassy silicates can alter the silicate's viscosity because they act as a flux and glass-network-modifier, respectively, which can subsequently alter creep performance.

3.2. Creep performance

The change in measured specimen height before and after creep testing correlated very well with the axial contraction measured with the contacting extensometer for all tested specimens. The deformation of refractories are frequently measured continuously during compressive creep testing using two (sometimes more) linear variable differential transducers whose mutual displacements coincide with the continuous position of the specimen ends [4]. The creep results generated from this technique are accurate only as long as the accumulated measured deformation coincides with the actual specimen heights measured before and after testing. Deformation and/or translation of the load train during the creep testing of the specimen, reaction of the specimen ends with the fixturing, and "bedding-down" of the specimen all have been shown to cause a lack of correlation between the measured deformation during testing and the change in pre- and post-test specimen height [15]. If any of these events are occurring then the measured contraction during testing is not solely due to creep. Consequently, caution must be exercised when interpreting deformation data generated using this technique because it will only be representative creep data if the experimenter verified and correlated pre- and post-test specimen height with the accumulated measured deformation. The advantage of the high temperature contacting extensometry used in the present study is that its accurate operation is independent of any rigid body motion or deformation of the test hardware, specimen, and push rod.

An interesting phenomenon was observed during the initial 15 to 20 hour soak. Note the contraction in Fig. 4 during the first 19.8 hours even at the low applied stress. This contraction is believed to be due to the continuation of sintering and/or some microstructural rearrangement occurring in the material due to an equilibrium state not being achieved during the material's fabrication. All the refractories exhibited this behavior to some extent, and the amounts for each are summarized in Table VI. These contraction effects were most dramatic in materials B, C, and D, and especially in materials C and D. For soak durations less than 18 hours, the contraction was

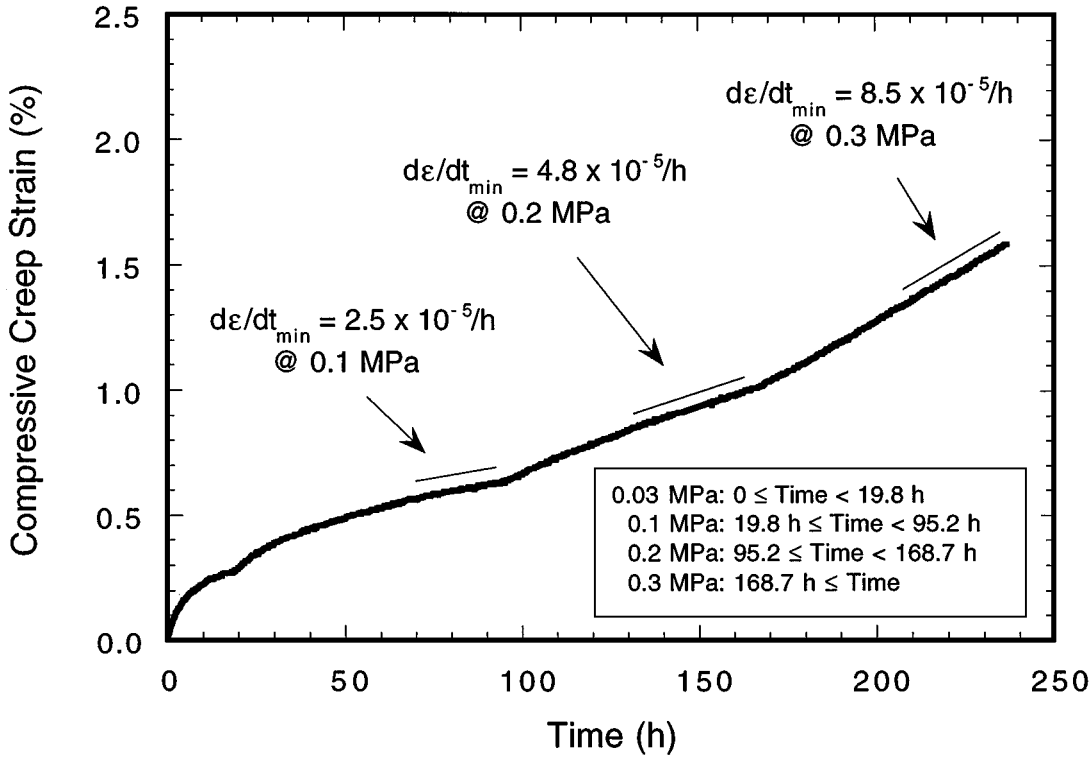

Figure 4 Example of a typical measured creep history. The shown strain-time profile was generated with material B at 1550 °C.

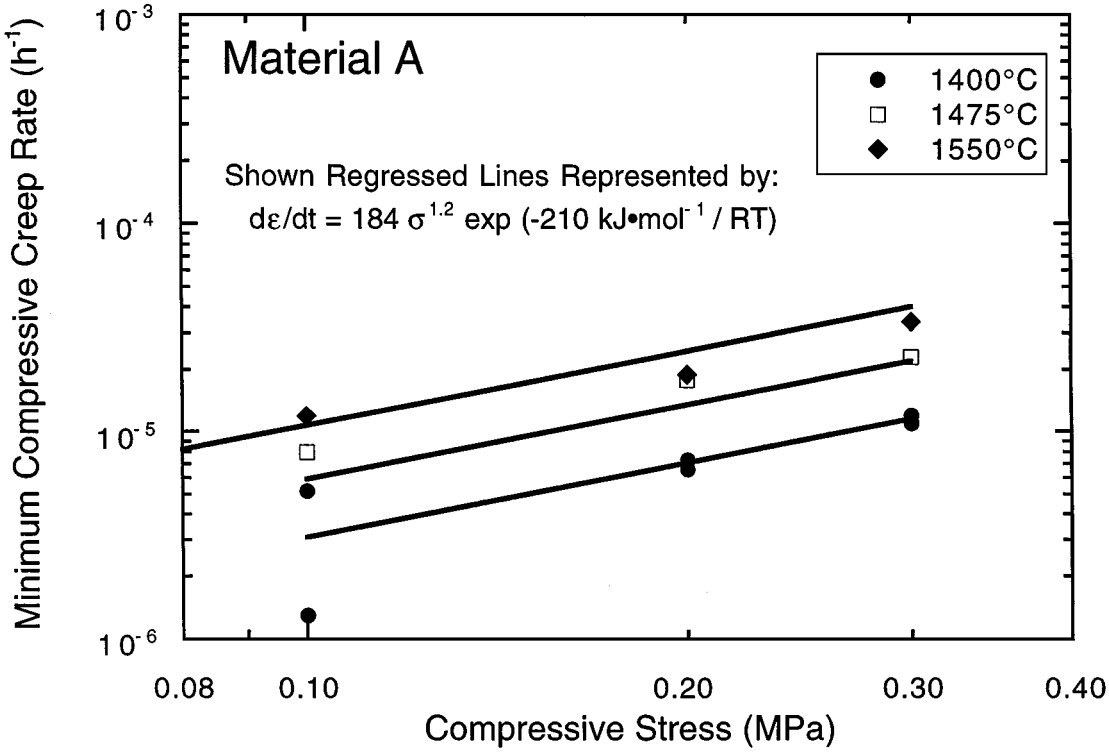

Figure 5 Creep rate as a function of stress for MgO material A.

TABLE VI Percent of contraction of MgO refractory prior to the application of the first test compressive stress[a]

MgO refractory ID	1400 °C or 2550 °F (hours[b])	1475 °C or 2685 °F (hours[b])	1550 °C or 2820 °F (hours[b])
A	DNM	DNM	0.02 ± 0.01[d] (13)
B	DNM	0.2 ± 0.05[c] (20)	0.27 ± 0.01[d] (20)
C	DNM	0.2 ± 0.05[c] (20)	0.38 ± 0.01[d] (18)
D	DNM	0.31 ± 0.01[d] (17)	0.35 ± 0.01[d] (18)
E	DNM	0.02 ± 0.01[d] (15)	0.04 ± 0.01[d] (18)

[a]A "low" compressive stress was actually applied (≈4 psi) during this test segment; it was used to maintain a slight preload in the specimen and the testframe's load train.
[b]Duration for the amount of shown contraction.
[c]This accuracy reflects that the contraction was estimated from a chart recorder.
[d]This accuracy reflects that the contraction was measured with the contacting extensometer.
DNM = Did Not Measure. The contraction was not experimentally measured for this condition; *however, this does not necessarily mean that no contraction occurred.*

more than 0.25% in material B and more than 0.35% in materials C and D. As will be seen, the measured creep rates for these two materials were quite high for the lowest applied stress (which also happened to be the first applied stress), so it was believed that this "time-hardening" effect was contributing to the measured creep deformation with the result being an apparently fast net creep rate. This information is valuable for it illustrates that a superstructure which is several feet in size will in fact significantly contract solely due to materials B, C, and D's initial exposure to temperatures equal to and greater than 1475 °C. Materials A and E also showed this contraction effect, but at more than an order of magnitude less than materials B, C, and D.

The general appearances of the creep curves were similar for each of the five brands. Typically, a region of primary creep lasting 20 to 40 hours was followed by a longer duration of slowly decreasing creep rate. Tertiary creep (i.e., an increasing creep rate) was never observed. An example of a typical creep curve is shown in Fig. 4. In many instances, a steady-state or constant creep rate was never achieved; consequently, the continuing transient nature of many of the creep rates resulted in a minimum (and not steady-state) creep rate being defined. A minimum creep rate was determined as a function of stress and temperature for each of the five brands.

After the minimum creep rates were determined, their values were related to the applied compressive stress and test temperature using the Arrhenius power law equation shown in Equation 1. A regression fit was made to the creep rate-stress data for all five brands, and the results for each are respectively illustrated in Figs 5–9. The values of the parameters A, n, and Q for each brand are tabulated in Table VII.

Using the parameters in Table VII, the relative creep resistances of the five refractories may be compared. For example, the minimum creep rates at 0.2 MPa and 1500 °C (2730 °F) would be: 1.7×10^{-5}/h for material A; 3.6×10^{-5}/h for material B; 4.8×10^{-5}/h for material C; 6.2×10^{-5}/h for material D; and 2.9×10^{-5}/h for material E. This shows material A was the most creep resistant MgO refractory, followed in order of creep resistance by materials E, B, C, and D. A refractory vendor* empirically defines deformation in checker packing exceeding 5% over 800 hours as being potentially problematic [16]. Using this criterion for

* Not necessarily one of the vendors of the MgO refractories tested in the present study.

TABLE VII Values of power law multilinear regression fit ($d\varepsilon/dt_{min} = A\sigma^n \exp(-Q/RT)$, where $d\varepsilon/dt_{min}$ has units of h^{-1})

MgO refractory ID	Pre-exponential constant A	Creep rate stress exponent n	Activation energy Q
A	184	1.2	210 kJ/mol = 50 kcal/mol
B	5.31×10^{-4}	0.9	290 kJ/mol = 69 kcal/mol
C	5.44×10^{-4}	0.5	24 kJ/mol = 5.7 kcal/mol
D	1.53×10^{-4}	0.1	11 kJ/mol = 2.6 kcal/mol
E	190	0.9	210 kJ/mol = 50 kcal/mol

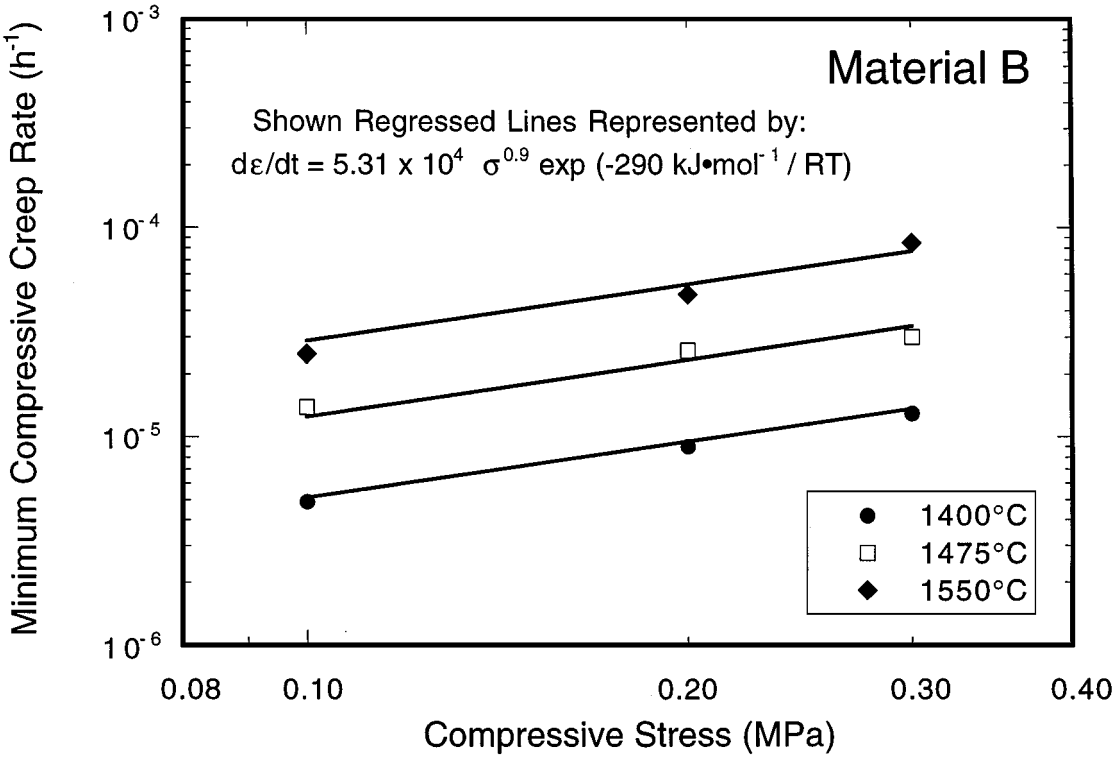

Figure 6 Creep rate as a function of stress for MgO material B.

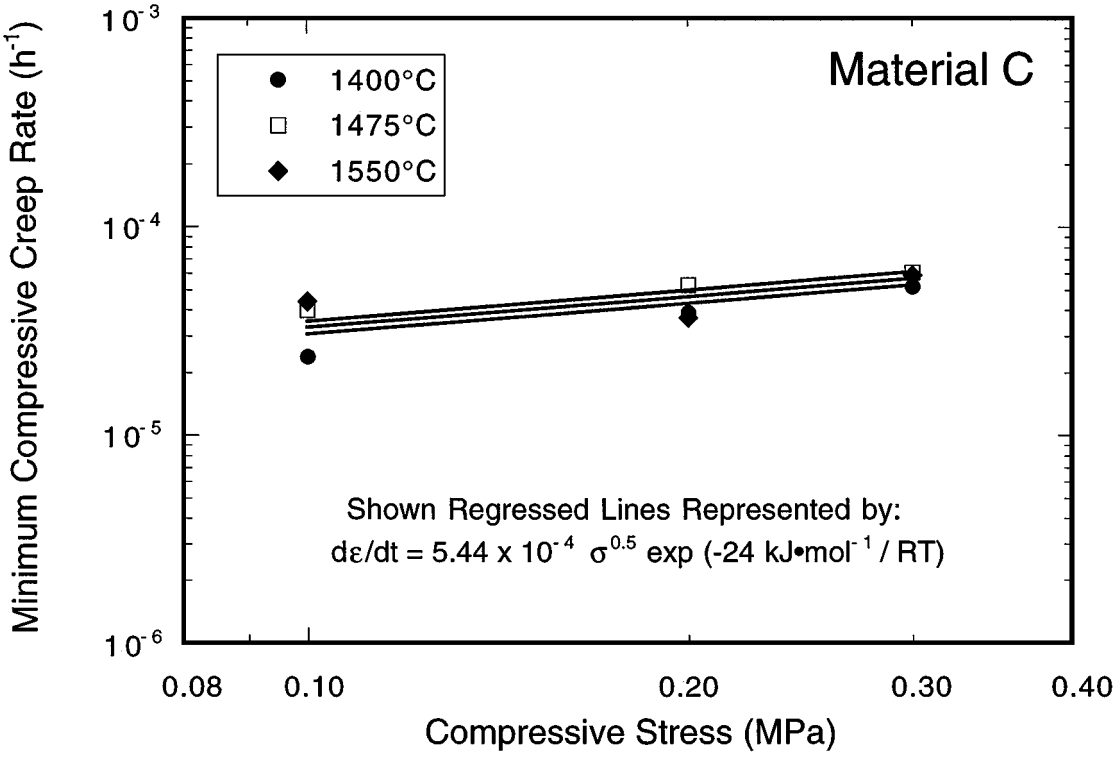

Figure 7 Creep rate as a function of stress for MgO material C.

the 1500 °C – 0.2 MPa example, and simply determining the product of 800 hours and the minimum creep rate for each refractory, material A would deform 1.4%; material B 2.9%; material C 3.8%; material D 5.0%; and material E 2.3%. All five brands would be acceptable under such a temperature and stress loading condition; however, this conclusion would not necessarily hold true for all five brands if they were subjected to the combination of a service temperature and stress greater than 1500 °C and 0.2 MPa.

In an effort to understand why the five MgO refractory brands crept so differently, phase changes brought on by the creep testing conditions were first compared to the as-received state of the materials. A specimen of each brand tested at 1550 °C was sectioned in half and metallographically polished. These 1550 °C specimens were chosen because they represented the severest temperature condition that each brand was subjected to (each of these creep specimens were at 1550 °C for approximately 250 hours). X-ray diffraction was then performed on the sectioned surface. The XRD results are shown in Table VIII and may be compared to the as-received material XRD results shown in Table IV. All five brands still showed the presence of Periclase, magnesium silicate, and tricalcium silicate. Unlike materials B, C, D, and E, material A did not have dicalcium silicate. Materials B, C, and D had Merwinite or Monticellite in their as-received state; however, these phases were no longer present after the 1550 °C creep testing. Lastly, material D changed from having forsterite and an undetermined phase (peak at $2\theta = 27.36^\circ$) in its as-received state to having Rankinite and a different undetermined phase (peak at $2\theta = 34.20^\circ$) after its 1550 °C testing. Wollastonite, Akermanite, Bredigite, or Brucite were not present in any of the five brands after testing (like their as-received state). The comparison of the XRD results before and after testing do not provide a definitive explanation of the order of creep resistance of the five brands; however, they provide some insight as to why materials B, C, and D were perhaps not as creep resistant as materials A and E. Materials B, C, and D in their as-received state had Merwinite or Monticellite, which are phases having relatively low liquidus temperatures (see Fig. 3a). This information suggests that the larger amounts of contraction (see Table VI) which these three brands exhibited during the initial 15–20 hour soak at 1475 and 1550 °C were an effect of the Merwinite or Monticellite phases present in these materials. Lastly, the least creep resistant material, material D, contained unknown phases in its as-received and 1550 °C tested states. The likelihood of these unknown phases having higher liquidus temperatures than the phases depicted in the ternary phase diagram of Fig. 3a is possible. Although it cannot be

TABLE VIII Phase analysis of Materials Creep Tested at 1550 °C (2820 °F). Specimens were at temperature for approximately 250 h

	Material				
Phase[a]	A	B	C	D	E
Periclase MgO PDF#45-0946	×	×	×	×	×
Magnesium silicate $MgO{\cdot}SiO_2$ PDF#34-1216 Forsterite $2MgO{\cdot}SiO_2$ PDF#35-0590	×	×	×	×	×
Dicalcium silicate $2CaO{\cdot}SiO_2$ PDF#31-0297		× (weak & diffuse)	× (weak & diffuse)	× (weak & diffuse)	× (weak & diffuse)
Tricalcium silicate $3CaO{\cdot}SiO_2$ PDF#31-0301	× (diffuse)	× (diffuse)	× (diffuse)	× (diffuse)	× (diffuse)
Rankinite $3CaO{\cdot}2SiO_2$ PDF#22-0539				× (weak & diffuse)	
Monticellite $CaO{\cdot}MgO{\cdot}SiO_2$ PDF#35-0590 or Merwinite $3CaO{\cdot}MgO{\cdot}2SiO_2$ PDF#35-0591[b]					
Undetermined peak at $2\theta = 27.36^\circ$					
Undetermined peak at $2\theta = 34.20^\circ$				× (weak & diffuse)	

[a]These phases were also sought but were not found: Lime (CaO – PDF#37-1497); Wollastonite ($CaO{\cdot}SiO_2$ – PDF#43-1460); Akermanite ($2CaO{\cdot}MgO{\cdot}2SiO_2$ – PDF#35-0592); Bredigite ($14CaO{\cdot}MgO{\cdot}8SiO_2$ – PDF#36-0399); and Brucite ($Mg(OH)_2$ – PDF#07-0239).
[b]The primary peaks for these two phases are similar and were indistinguishable because their intensities were low-valued and diffuse.

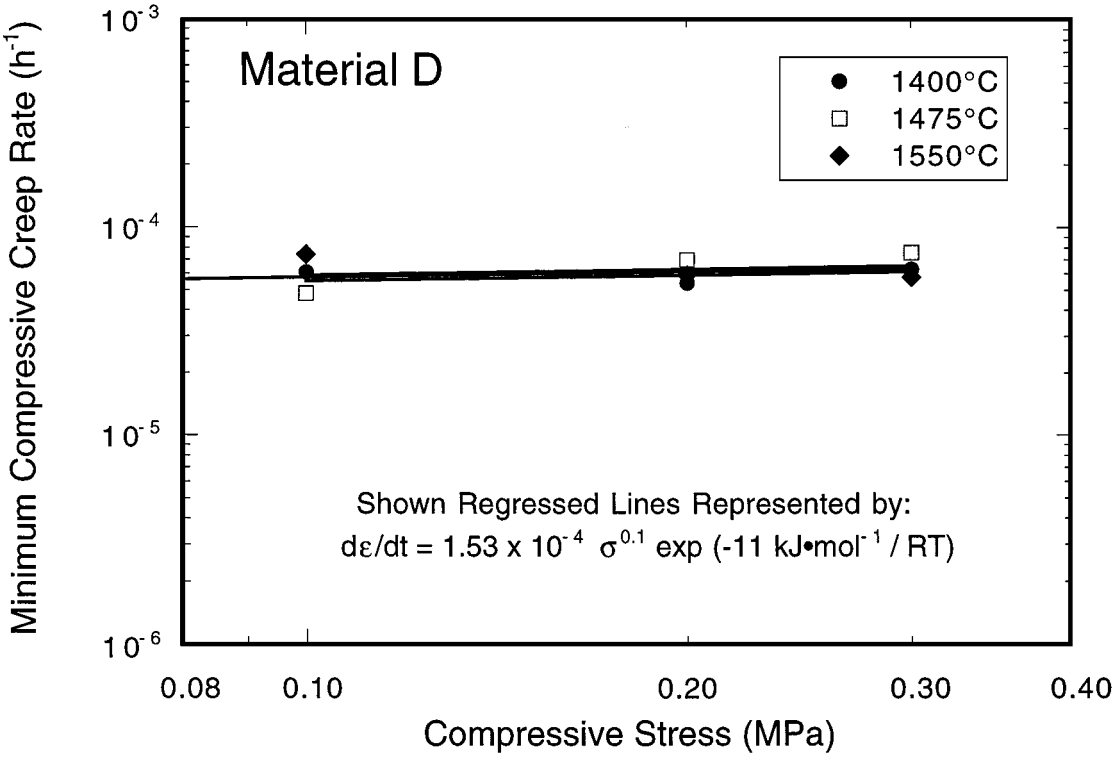

Figure 8 Creep rate as a function of stress for MgO material D.

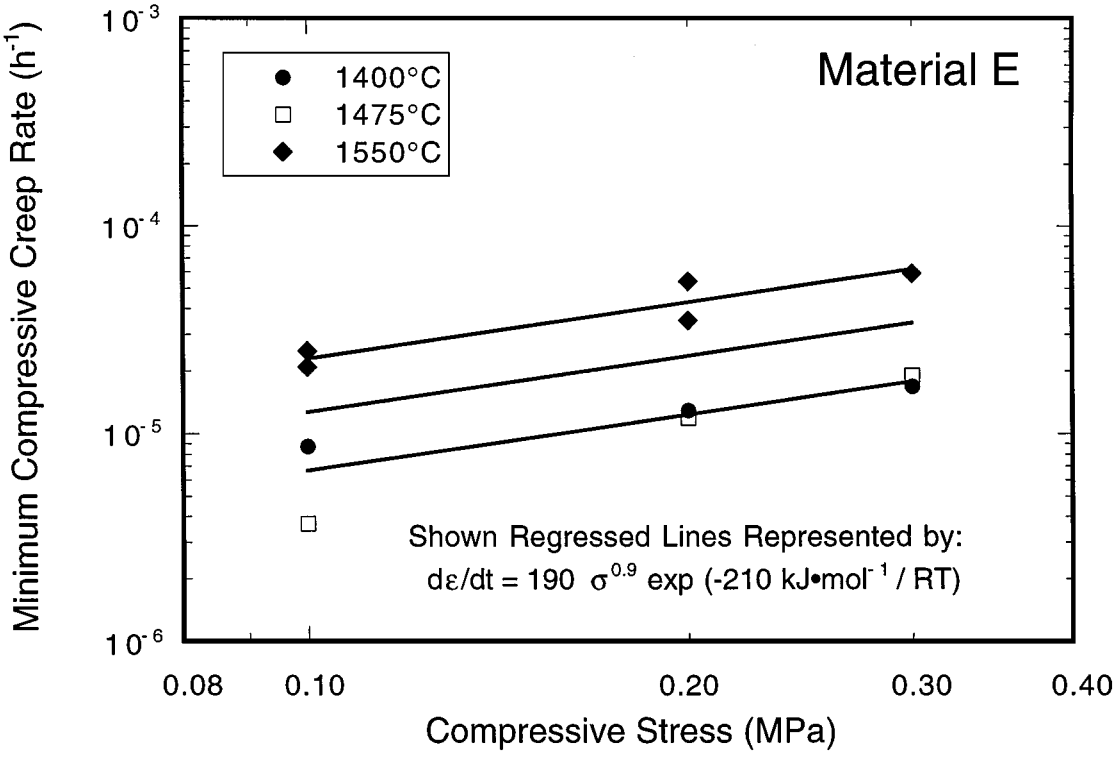

Figure 9 Creep rate as a function of stress for MgO material E.

concluded that these unknown phases were responsible for material D having the worst creep resistance among the five brands, it can be concluded that their presence did not benefit material D's creep resistance.

Other differences in the pre-test character of the five brands were also examined. Higher levels of porosity have been shown to increase bulk creep rates in polycrystalline ceramics [3, 17], so the equivalent levels of porosity in the five brands do not account for the differing creep resistances between them. The change in porosity in MgO refractories has been shown not to significantly change with compressive creep during testing [18], so the amount of as-received porosity in the five brands tested in the present study perhaps did not appreciably change as a consequence of the creep testing.

Materials A and E had significantly larger average grain sizes than materials B, C, and D (see Table III).

With polycrystalline ceramics, creep rate is inversely proportional to the square of grain size for Nabarro-Herring creep or to the cube of diameter for Coble creep [19]. As a consequence, a larger grain size will tend to decrease the creep rate.

In general, narrower grain size distributions promote close-packing, and this may be potentially problematic to creep resistance. Close-packed systems are dilatant (i.e., the particles assume a less dense mode of packing when the body is sheared) and the deformation is dependent on the cohesive force between particles [20]. The cohesive force between particles in polycrystalline ceramics is dependent on the wetting behavior of the glassy secondary phase and its viscosity. Consequently, a wider grain size distribution (as in the case of material E) is less prone to dilatant behavior, so its overall deformation behavior is not as dependent on the viscosity of the glassy secondary phase as it would be for a polycrystalline ceramic with a narrow agglomerate size distribution. Compared to materials B, C, and D, material E had an equivalent porosity and a relatively low CaO/SiO_2 wt % ratio, yet its creep resistance was better than the others. Material E's large average grain size and wide size distribution may have contributed to its better creep resistance. Although the grain size and distribution were reported to have a negligible effect on the creep of a 99.85% MgO refractory up to 1500 °C at compressive stresses up to 4.3 MPa (630 psi) [6], the results from the present study do not necessarily support the findings those authors observed. Although it is not fully understood why these findings are contradictory, the five brands examined in the present study contained larger volume fractions of secondary phases. The grains in these five brands may have been able to slide and mutually displace more than if little or no secondary phase was different.

Although the grain shapes were not quantified, it was observed that many of their grains were non-equiaxed in shape. In fact, many grains were relatively long or needle-shaped. Interlocking or pinning of equiaxed grains by networked, acicular grains has been shown to improve creep resistance [21] in polycrystalline ceramics. Creep resistance is even further improved if the equiaxed grains are larger within this mixture of acicular-shaped grains [22]. Consequently, the elongated or acicular-shaped grains in materials A and E may have contributed to their better creep resistance.

Impurity content may have affected creep resistance as well. Material D (the least creep resistant among the five brands) had a high iron content relative to materials A, B, C, and E. Consistent with the relatively high iron content and poor creep resistance in material D, it has been reported [23] that larger iron contents have been responsible for faster creep rates in other MgO refractories. Boron also has been shown to lessen the creep resistance of MgO refractories [24] at levels as low as 500 ppm (0.05%). The EDS results in the present study did not show any evidence of boron at concentrations greater than 100 ppm in any of the five brands. It may be concluded then that boron, and its potentially detrimental effects on creep resistance, did not contribute to the creep behavior of any of the MgO brands tested in the present study.

3.3. Designing a creep resistant CaO/SiO_2-containing MgO refractory

The results from the present study suggest that there are several criteria which need to be satisfied in order to obtain a CaO/SiO_2-containing MgO refractory with optimum creep resistance. Material A was the most creep resistant MgO refractory among the five brands tested, so its combination of microstructural, chemical, and physical properties serve as the best initial model of a hypothetically new and improved MgO refractory. A hypothetical CaO/SiO_2-containing MgO refractory with maximum creep resistance would have the combination of (1) a relatively high MgO content, (2) minimal porosity, (3) a relatively large average grain size, (4) a relatively wide grain size distribution, (5) some elongated or acicular-shaped grains, (6) no $CaO{\cdot}MgO{\cdot}SiO_2$ ternary phases, (7) a relatively high CaO/SiO_2 wt % ratio, and (8) an iron impurity content less than 100 ppm. Additionally, firing temperature should be sufficiently high for all sintering reactions to be completed prior to service. Lastly, it may be inferred that the creep resistance of this hypothetical MgO refractory will also be maximized if impurity concentrations of sodium, aluminum, and boron are kept to a minimum.

3.4. Stress exponents, activation energies, and creep mechanisms

The determined stress exponents for materials A, B, and E were approximately equal to one, which is indicative of the dominance (or rate-controlling) of a diffusion or Coble creep mechanism [19]. The relatively low values of the stress exponents for materials C and D are peculiar; however, their low values are believed to be: (1) a direct consequence of the contraction or time-hardening effects which were represented in Table VI and (2) an negative consequence of the assumption that a single deformation mechanism was active at all temperatures and stresses. Such low values for other MgO refractories have been reported in the literature [16]. The activity of the contraction mechanism at 1475 °C and above was time-dependent (i.e., independent of stress) and perhaps lasted for many tens of hours before an equilibrium state was achieved. Materials C and D (and material B to a lesser extent) strongly exhibited this contraction effect (see Table VI). The measured creep rates for the 0.1 MPa loadings of materials C and D appeared to be relatively fast (compared to the subsequent measured creep rates at 0.2 and 0.3 MPa). This observation was attributed to the likelihood that both materials C and D: (1) crept due to the application of the 0.1 MPa compressive stress and (2) were still experiencing time-hardening effects. For materials C and D, the contraction or time-hardening effects were still active even at the 0.2 MPa (i.e., after 100 hours at temperature) loadings. The consequence of these two mechanisms being active on the multilinear regression

was that the analysis yielded an apparently low-valued stress exponent for these two brands. Reiterating, the use of this multilinear regression algorithm assumes that a single rate-controlling mechanism is dominant for all temperatures and stresses: the observation that two mechanisms were active during early test times suggests that the single-acting-mechanism assumption was invalid for materials C and D.

The range of activation energies (50–70 kcal/mol) for materials A, B, and E is consistent with activation energy values reported for other calcium-silicate MgO refractories in the literature [2–4, 6, 7, 25], and is equivalent to the activation energy for viscous flow in a silicate melt [26]. Similar to the anomalously-low stress exponents for materials C and D, the activation energies shown in Table VII for these same materials reiterates the invalidation of the single-acting-mechanism assumption for the usage of Equation 1. The illustration of the relative values of these activation energies are depicted in Figs 5–9. The larger valued activation energies for materials A, B, and E are illustrated by the relatively wide gaps between the fitted lines (i.e., temperatures) in Figs 5, 6, and 9, respectively. However, the low-valued activation energy values for materials C and D results in a collapsing of the creep data in Figs 7–8 indicating that there was very little temperature dependence on creep deformation in these two brands.

4. Conclusions

Compressive creep tests were conducted on five commercially-available brands of CaO/SiO_2-containing MgO refractories between 1400 and 1550 °C in ambient air using static compressive stresses between 0.10 and 0.30 MPa. Creep resistance was found to vary among the five brands. Some of the brands significantly contracted even at a negligible stress at 1550 °C. The relative amounts of porosity, impurities, types of phases present, and the grain size distribution were found to affect creep resistance, so the higher MgO contents and CaO/SiO_2 wt % ratios in of themselves were not necessarily indicators of the better creep resistance among these brands. The more creep resistant brands tended to have a combination of: (1) a larger average grain size and wider size distribution, (2) a low iron content, and (3) an absence of CaO-MgO-SiO_2 ternary compounds. Creep rates of three brands were well-represented by a power-law creep formulation. The values of the determined creep-stress exponents for these brands suggested their compressive creep was dominated (or rate-controlled) by a diffusion mechanism, while the values of the determined activation energies suggested that creep in these MgO brands was accommodated by grain boundary sliding through viscous deformation of the calcium silicate grain-boundary phase. Two brands not well-represented by a power-law creep formulation showed relatively dramatic time-hardening behavior, which frustrated the understanding of stress-dependence on their creep deformation.

Acknowledgements

The authors wish to thank C. R. Brinkman and K. C. Liu of ORNL and R. E. Moore of the University of Missouri-Rolla for reviewing the manuscript and for their helpful comments. Gratitude is also expressed toward H.-T. Lin, S. B. Waters, and T. R. Watkins for their assistance with the EDS and XRD characterization.

References

1. S. V. GILBERT and J. E. MOORE, *Glass Ind*. September (1988) 26.
2. W. E. SNOWDEN and J. A. PASK, *J. Amer. Ceram. Soc*. **61** (1978) 231.
3. P. J. DIXON-STUBBS and B. WILSHIRE, *Trans. J. Br. Ceram. Soc*. **79** (1980) 21.
4. P. J. DIXON-STUBBS and B. WILSHIRE, *ibid*. **80** (1981) 180.
5. R. K. GHOSE and J. WHITE, *ibid*. **79** (1980) 146.
6. R. W. EVANS, P. J. SCHARNING and B. WILSHIRE, *ibid*. **84** (1985) 108.
7. T. VASILOS, F. B. MITCHELL and R. M. SPRIGGS, *Science of Sintering* **18** (1986) 65.
8. G. R. EUSNER and W. H. SCHAEFFER, Jr., *Ceram. Bull*. **35** (1956) 265.
9. Standard test methods for apparent porosity, water absorption, apparent specific gravity, and bulk density of burned refractory brick and shapes by boiling water, ASTM C20, Vol. 15.01, "Annual Book of ASTM Standards" (ASTM, West Conshohocken, PA, 1996).
10. S. SHIN and O. BUYUKOZTURK, Material property development for refractories, U.S. DOE Report ORNL/Sub/79-07862/02, 1990.
11. Standard test method of measuring the thermal expansion and creep of refractories under load, ASTM C832, Vol. 15.01, "Annual Book of ASTM Standards" (ASTM, West Conshohocken, PA, 1996).
12. F. H. NORTON, "The Creep of Steel at High Temperature" (McGraw Hill, New York, 1929).
13. MgO-CaO-SiO_2 Ternary Phase Diagram, Fig. 598, "Phase Diagrams for Ceramists" (American Ceramic Society, Columbus, OH, 1964).
14. CaO-SiO_2 Binary Phase Diagram, Fig. 237, "Phase Diagrams for Ceramists" (American Ceramic Society, Columbus, OH, 1964).
15. J. F. CLEMENTS and J. VYSE, *Trans. J. Br. Ceram. Soc*. **65** (1966) 59.
16. S. V. GILBERT, *Glass Ind*. September (1985) 14.
17. P. BOCH and J. C. GLANDUS, *Interceram* (3) (1983) 33.
18. I. I. VISHNEVSKII, A. V. KUSHCHENKO, L. D. SMIRNOVA, R. E. VOL'FSON and G. N. SHCHERBENKO, *Ogneupory* **6** (1986) 4.
19. W. R. CANNON and T. G. LANGDON, *J. Mater. Sci*. **18** (1983) 1–50.
20. E. B. ALLISON, P. BROCK and J. WHITE, *Trans. J. Br. Ceram. Soc*. **58** (1959) 495.
21. H.-T. LIN and P. F. BECHER, *J. Amer. Ceram. Soc*. **74** (1991) 1886.
22. H.-T. LIN, K. B. ALEXANDER and P. F. BECHER, *J. Amer. Ceram. Soc*. **79** (1996) 1530.
23. R. W. EVANS, P. J. SCHARNING and B. WILSHIRE, *J. Mater. Sci*. **20** (1985) 4163.
24. G. E. SHAFFER, Compressive creep of magnesia refractories, M.S. thesis, The Pennsylvania State University, University Park, PA, 1973.
25. R. F. KRAUSE, Jr., *Ceram. Eng. Sci. Proc*. **7** (1986) 220.
26. P. RICHET, *Geochim. Cosmochim. Acta*. **48** (1984) 471.

Received 3 September
and accepted 22 September 1998